Neuron, Vol. 25, 43–56, January, 2000, Copyright ©2000 by Cell Press

Neuropilin-2 Regulates the Development of Select Cranial and Sensory Nerves and Hippocampal Mossy Fiber Projections

Hang Chen,* Anil Bagri,*† Joel A. Zupicich,§ Yimin Zou,* Esther Stoeckli,‖ Samuel J. Pleasure,*† Daniel H. Lowenstein,† William C. Skarnes,§ Alain Chédotal,#‡ and Marc Tessier-Lavigne*#

*Department of Anatomy
Department of Biochemistry and Biophysics
Howard Hughes Medical Institute
University of California
San Francisco, California 94243-0452
†Department of Neurology
University of California
San Francisco, California 94243-0014
‡INSERM U106
Bâtiment de Pédiatrie
Hôpital de la Salpétrière
47 Boulevard de l'Hôpital
75013 Paris
France
§Department of Molecular and Cell Biology
University of California
Berkeley, California 94720
‖Department of Integrative Biology
University of Basel
Rheinsprung 9
CH-4051 Basel
Switzerland

Summary

Neuropilin-1 and neuropilin-2 bind differentially to different class 3 semaphorins and are thought to provide the ligand-binding moieties in receptor complexes mediating repulsive responses to these semaphorins. Here, we have studied the function of neuropilin-2 through analysis of a neuropilin-2 mutant mouse, which is viable and fertile. Repulsive responses of sympathetic and hippocampal neurons to Sema3F but not to Sema3A are abolished in the mutant. Marked defects are observed in the development of several cranial nerves, in the initial central projections of spinal sensory axons, and in the anterior commissure, habenulo-interpeduncular tract, and the projections of hippocampal mossy fiber axons in the infrapyramidal bundle. Our results show that neuropilin-2 is an essential component of the Sema3F receptor and identify key roles for neuropilin-2 in axon guidance in the PNS and CNS.

Introduction

The projection of developing axons to their proper targets is an essential step in establishing appropriate neuronal connections. Axonal pathfinding is guided by the coordinate action of attractive and repulsive mechanisms (Tessier-Lavigne and Goodman, 1996). One large family of secreted and transmembrane proteins that function in repulsion are the semaphorins, which are characterized by the presence of a conserved ~500 amino acid semaphorin (sema) domain at their amino termini (reviewed in Kolodkin, 1998). The semaphorins are divided into seven subfamilies based on the other types of motifs they possess (Semaphorin Nomenclature Committee, 1999). The best-characterized vertebrate semaphorins are those in class 3, with six known members (Sema3A–Sema3F). These semaphorins have been shown to be chemorepulsive molecules, able to induce growth cone collapse when applied acutely and uniformly and to steer axons away when presented as a point source; some secreted and transmembrane semaphorins have also been reported to act as chemoattractants (reviewed in Kolodkin, 1998; Chisholm and Tessier-Lavigne, 1999).

The receptor mechanisms that mediate the repulsive actions of class 3 semaphorins have been the subject of intense study over the past several years. The evidence to date indicates that individual class 3 semaphorin receptors are complexes formed from members of two transmembrane receptor families, neuropilins and plexins. Plexins appear to be receptors for several other classes of semaphorins (classes 2, 4, and 7) in invertebrates and vertebrates (Comeau et al., 1998; Winberg et al., 1998; Tamagnone et al., 1999), apparently functioning directly to bind those semaphorins. In the case of class 3 semaphorins, however, plexins appear to provide only a signaling moiety in a receptor complex (Takahashi et al., 1999; Tamagnone et al., 1999), with ligand binding mediated by members of the neuropilin family, neuropilin-1 and -2 (Chen et al., 1997; He and Tessier-Lavigne, 1997; Kolodkin et al., 1997).

The neuropilins are a small family of transmembrane proteins implicated in a variety of biological functions (Chen et al., 1997; He and Tessier-Lavigne, 1997; Kitsukawa et al., 1997; Kolodkin et al., 1997, 1998; Soker et al., 1998; Kawasaki et al., 1999). The first characterized member, neuropilin-1, was originally identified as a cell surface antigen expressed in the *Xenopus laevis* retinotectal system (Takagi et al., 1991). Neuropilin-1 homologs were later isolated in chick (Takagi et al., 1995), mouse (Kawakami et al., 1996), rat, and human (He and Tessier-Lavigne, 1997; Kolodkin et al., 1997). Neuropilin-2 was identified as second member of the neuropilin family (Chen et al., 1997; Kolodkin et al., 1997). The extracellular domain of neuropilins consists of five structural domains sharing homology with other known proteins: two CUB motifs (domains a1 and a2), two domains of homology to coagulation factors V and VIII (domains b1 and b2), and a MAM domain ([domain c]; Takagi et al., 1991; Kawakami et al., 1996; Chen et al., 1997). Neuropilin-2 is about 44% identical to neuropilin-1 at the amino acid level, and there are at least six splice variants of neuropilin-2 differing in their transmembrane and cytoplasmic domains. The two main neuropilin-2 isoforms, called 2a and 2b, show only 10% identity in

#To whom correspondence should be addressed (e-mail: marctl@itsa.ucsf.edu [M. T.-L.], chedotal@infobiogen.fr [A. C.]).

the alternatively spliced regions (Chen et al., 1997). The cytoplasmic region of neuropilins is short (about 40 amino acids) and contains no signal transduction motifs.

Different class 3 semaphorins bind neuropilin-1 and neuropilin-2 with different affinities, with Sema3A binding neuropilin-1 but not neuropilin-2 with high affinity, Sema3F binding neuropilin-2 with much higher affinity than neuropilin-1, and Sema3C binding the two with similar affinities (Chen et al., 1997). This has led to the suggestion that the Sema3A signal is mediated by a receptor involving principally neuropilin-1, the Sema3F signal by a receptor involving principally neuropilin-2, and the Sema3C signal by a receptor involving either neuropilin-2 or both neuropilin-1 and neuropilin-2 (Chen et al., 1997). Support for this model was provided first by experiments using antibodies to neuropilin-1, as well as neurons derived from a neuropilin-1 knockout mouse, which showed that neuropilin-1 is essential to Sema3A function (He and Tessier-Lavigne, 1997; Kitsukawa et al., 1997; Kolodkin et al., 1997). More recently, the evidence has also supported the suggestion that neuropilin-2 is a functional receptor for Sema3F (Chédotal et al., 1998; Chen et al., 1998; Giger et al., 1998; Takahashi et al., 1998).

The two neuropilins are broadly expressed in embryonic and adult organs, often in complementary patterns, and are particularly abundant in the central nervous system (CNS) (Kawakami et al 1996; Chen et al., 1997; Chédotal et al., 1998). Analysis of a neuropilin-1 knockout mouse (Kitsukawa et al., 1997) has demonstrated an essential role for neuropilin-1 in pathfinding of several populations of peripheral sensory neurons. The observed phenotypes and their similarity to phenotypes observed in a Sema3A knockout mouse (Taniguchi et al., 1997) suggested that Sema3A, acting via neuropilin-1, was functioning to guide these axonal populations through providing barriers to growth of some of the axons, as well as through surround repulsion. More recently, neuropilin-1 has also been implicated in blood vessel formation, since neuropilin-1 is a receptor for several vascular endothelial growth factor isoforms, apparently functioning as a coreceptor with the Flk-1/KDR receptor tyrosine kinase (Migdal et al., 1998; Soker et al., 1998; Makinen et al., 1999), and since loss of neuropilin-1 function in mice leads to disruption of vessel formation and death of the embryos at mid-gestation (Kawasaki et al., 1999).

Whereas the function of neuropilin-1 is starting to be known in greater detail, little is known about the function of neuropilin-2. Studies of the expression patterns of neuropilin-2 and Sema3F have suggested a role in the guidance of hippocampal axons (Chédotal et al., 1998), but otherwise the potential role of neuropilin-2 in guidance of other axonal classes has not been defined. Neuropilin-2 is also a receptor for isoforms of vascular endothelial growth factor (Soker et al., 1998). To gain further insight into neuropilin-2 function in vivo, we have studied neuropilin-2 knockout mice that we isolated using a gene trap strategy. Here, we report an analysis of neuronal development and axonal trajectories in the mutant mice. Our results indicate that neuropilin-2 is indeed a necessary receptor for Sema3F and that neuropilin-2 plays important roles in establishing several axonal trajectories in the developing CNS and PNS.

Results

Generation of *neuropilin-2*-Deficient Mice

A mutation in the *neuropilin-2* locus in embryonic stem cells was isolated by gene trapping using the so-called "secretory trap vector," which encodes the transmembrane domain of CD4 and a β-galactosidase-neomycin fusion protein (β-geo) (Skarnes et al., 1995). As described, this vector can be used to selectively mutate genes encoding proteins with signal sequences. Mutation of such a gene is achieved by insertion into an intron in the gene in ES cells (described in Skarnes et al., 1995). Using this approach, an embryonic stem cell line (GST39) was recovered carrying an insertion of the gene trap vector in the *neuropilin-2* gene, as revealed by RT-PCR and 5′-RACE. The insertion site was found to be in an intron interrupting the *neuropilin-2* coding sequence at cDNA position 2069 nt (amino acid Pro-680), located one-third of the way into the MAM domain of neuropilin-2. The mutant allele was transmitted through the germline to generate mice heterozygous for the mutant allele, which were intercrossed to recover homozygous mutant progeny. The allele is predicted to be a loss-of-function allele for two reasons. First, with this gene trap vector, the chimeric proteins resulting from the fusion of the upstream sequences with the vector sequences appear to be localized to an intracellular compartment rather than presented on the cell surface, apparently due to sequences within the targeting vector (Skarnes et al., 1995). Second, the MAM domain of neuropilin-1 has been shown to be essential for its function as a functional semaphorin receptor (Giger et al., 1998; Nakamura et al., 1998), and it is expected that the same will be true of neuropilin-2, further indicating that the targeted allele is likely to be a loss-of-function allele.

The genotype of embryos, as well as the relative levels of wild-type and fusion transcripts in embryonic and adult mice, were determined by RT-PCR using a triprimer method, as shown in Figure 1A. β-galactosidase staining of embryos and dot-blot analysis of genomic DNA with a fragment of the β-galactosidase probe confirmed the genotype determined by RT-PCR (data not shown). To determine whether the gene trap vector worked efficiently in splicing to upstream exons, RNase protection analysis was performed on total RNA extracted from wild-type, heterozygous, and homozygous embryos, using a 250 nucleotide probe (probe A) that covers the junction of the gene trap vector insertion site, as well as a 280 nucleotide probe that anneals to the 3′ most coding region of the *neuropilin-2* A-isoform (probe B). Wild-type transcripts were detected but only at a very low level, corresponding to about 0.5% of the fusion transcript, as shown in Figures 1B and 1C. Thus, as for a *netrin-1* knockout mouse generated by the same strategy (Serafini et al., 1996), it appears that the knockout mice generated here carry a severely hypomorphic, or near-null, allele of the *neuropilin-2* gene. Mice homozygous for this mutant allele appear viable, and homozygous males and females are fertile (although the average litter size for a homozygous female appears small (usually five or fewer embryos) (data not shown). We have not yet determined, however, whether all homozygous animals are fertile, as we are still in the process of attempting to breed a statistically significant number of

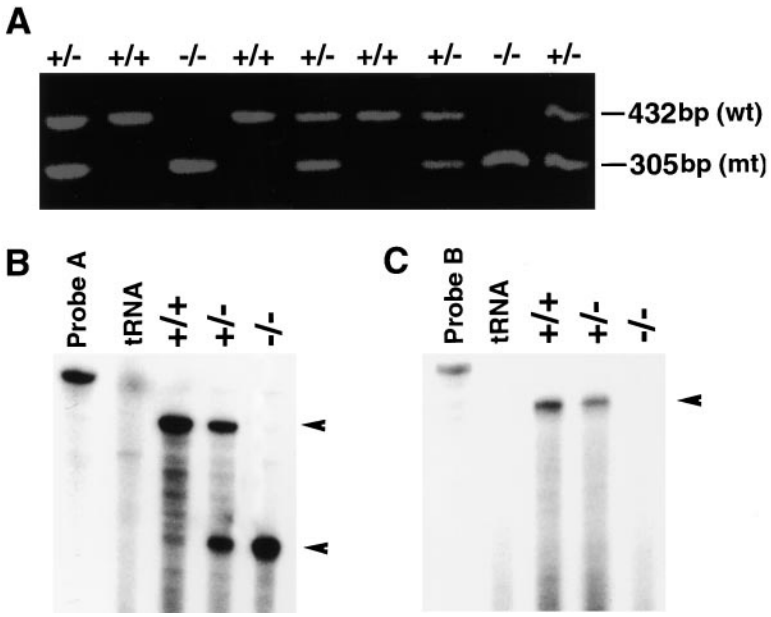

Figure 1. Characterization of the *neuropilin-2* Mutant Allele

(A) RT-PCR was performed on embryonic tissue using a triple primer set to amplify products corresponding to the wild-type (432 bp) and mutant (305 bp) genes. Genotypes determined by RT-PCR corresponded to those determined by dot blotting of genomic DNA.

(B) RNase protection assay with a 250-nucleotide ^{32}P-labeled riboprobe overlapping the insertion junction (probe A). Twenty micrograms total RNA extracts from wild-type (+/+), heterozygous (+/−), and mutant (−/−) mouse tissue were used to perform RNase protection assay, using yeast tRNA as negative control. The samples were analyzed on 7 M urea and 10% polyacrymide gel and quantified using a phosphoimager. Probe A, full-length probe; tRNA, yeast tRNA. The protected band corresponding to the full-length transcript is indicated by the top arrowhead. That corresponding to the mutant transcript is indicated by the bottom arrowhead. Homozygous mutant embryos show ~0.5% of the level of wild-type transcript seen in wild-type embryos.

(C) RNase protection assay with a ^{32}P-labeled riboprobe annealing to the 3′-end of the coding region of the neuropilin-2 A isoform cDNA. Arrowhead shows the protected fragment.

mutant adults to examine their fertility. The mutation was backcrossed to both CD1 and C57BL/6J backgrounds for at least five generations; the phenotypes described here were observed on both backgrounds.

To confirm that this mutant allele is a loss-of-function allele, we took advantage of the fact that neuropilin-2 is a necessary high-affinity receptor that mediates the repulsive action of Sema3F on sympathetic axons (Chen et al., 1998; Giger et al., 1998). We therefore tested the responses to Sema3F of superior cervical ganglia isolated from wild-type, heterozygous, and homozygous mutant embryonic day 13.5 (E13.5) embryos, using an in vitro coculture repulsion assay in a three-dimensional collagen matrix. Whereas strong repulsion of SCG axons from wild-type mice by Sema3F was observed, the response of SCG axons from heterozygotes was decreased relative to that from wild-type embryos, and the response of SCG axons from homozygous embryos was apparently abolished altogether (Figure 2). This reduction in responsiveness appeared to be specific, since responses to Sema3A, which are mediated by neuropilin-1 rather than neuropilin-2, were comparable in SCGs from homozygotes, heterozygotes, and wild-type embryos (Figure 2). These results confirm the prediction that the allele is a loss-of-function allele.

Abnormality of Cranial Nerve Trajectories

Neuropilin-2 is highly expressed in the nervous system of developing embryos and has a dynamic expression pattern that has been reported previously (Chen et al., 1997). We first examined whether there were any gross abnormalities in the morphology of tissues expressing *neuropilin-2*, taking advantage of the fact that the neuropilin-β-geo fusion protein is expressed in the cell bodies of neurons that normally express *neuropilin-2* and can be detected by β-galactosidase staining in heterozygotes and homozygotes. No gross defects in the overall morphology or placement of β-galactosidase stained cells was observed in cryostat sections from homozygous embryos compared to heterozygotes, including in sections through the trigeminal ganglion, trochlear nucleus, olfactory epithelium, and vomeronasal organs (Figure 3; data not shown). Furthermore, the expression pattern of *neuropilin-2* inferred from these β-galactosidase staining patterns corresponds precisely to the pattern of *neuropilin-2* transcripts detected previously by in situ hybridization (Chen et al., 1997).

To test for defects in axon guidance, we first focused on the patterns of projection of axons that pioneer the earliest nerve tracts in E10.5 and E11.5 embryos, which were revealed by whole-mount immunostaining using an antibody to neurofilament (NFM) (Figure 4). At E10.5, a pronounced defasciculation of the axons in the oculomotor nerve (cranial nerve III) was observed in homozygous embryos (Figure 4B) (six embryos from two litters), whereas those axons course as a tight bundle in wild-type (Figure 4A) and heterozygous (data not shown) embryos. The ophthalmic branch of the trigeminal nerve (cranial nerve V) also showed a mild defasiculation phenotype (Figure 4B). A more severe phenotype was observed for trochlear axons (which constitute the IVth cranial nerve). These axons originate in cell bodies located in the ventral region of the junction between midbrain and hindbrain and then project dorsally to the roof plate, where they cross the midline and exit the CNS, projecting to innervate the superior oblique muscle of the controlateral eye. At E11.5, these axons were observed projecting in a normal pattern in wild-type (Figure 4C) and heterozygous embryos (data not shown). Strikingly, however, no obvious trochlear motor nerve was observed in the homozygous mutant embryos (seven

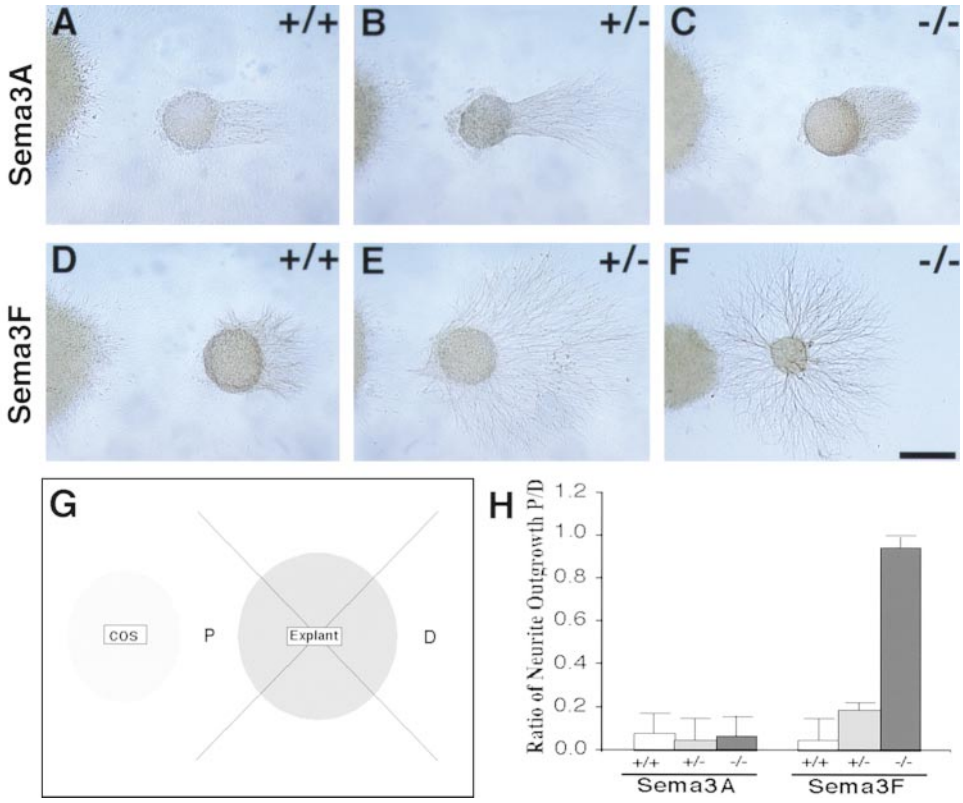

Figure 2. Neuropilin-2 Function Is Required for the Repulsive Action of Sema3F on Sympathetic Axons

SCG explants were dissected from E13.5 mouse embryos and cocultured with semaphorin-expressing COS 7 cell aggregates in a collagen matrix.

(A) through (C) Sema 3A repels sympathetic axons from wild-type (+/+), heterozygous (+/−), and mutant (−/−) embryos.

(D) through (F) Repulsion of sympathetic axons by Sema3F is reduced in heterozygotes and apparently abolished in the homozygotes.

(G and H) Quantitation of the repulsion experiments. (G) The extent of axon outgrowth on the side of the explant proximal to the source (length P) and the side distal to the source (length D) were measured. The axon outgrowth ratio P/D is a measure of repulsive activity, with a P/D ration of 1 indicating no repulsion. Bar shows means (± SEM) for each condition. For each condition, n = 20–24 explants from 8–10 embryos from four separate litters were used. SCG explants from mutant animals (−/−) do not respond to Sema 3F ($p < 0.0001$, Student's test), while those from heterozygous embryos show a reduced responsiveness to Sema 3F ($p < 0.0001$).

Scale bar for (A) through (H), 150 μm.

embryos from two litters) (Figures 4D). This phenotype could in principle result from an absence of the IVth nerve nuclei, misrouting of the axons, or severe defasciculation of the axons in the periphery (which might make the individual axons undetectable by whole-mount staining). The first explanation seems unlikely since β-galactosidase staining showed no obvious difference in the trochlear nuclei of heterozygous and homozygous embryos at E11 (Figures 3B and 3C), but we have not established whether the defect is due to the misrouting or defasciculation of the axons. The expression pattern of the high-affinity neuropilin-2 ligand Sema3F, which is localized both rostral and caudal to the mid-hindbrain junction where the trochlear axons travel, is consistent with the possibility that Sema3F creates an inhibitory surround that helps channel these axons along the mid-hindbrain junction (A. Kolodkin, D. Ginty, and colleagues, personal communication).

In contrast to these defects in the peripheral projections of cranial nerves, the peripheral projections of spinal sensory neurons and motor neurons appeared largely normal in the mutants, at least at the level of resolution afforded by whole-mount immunostaining on E12.5 embryos (data not shown), and by immunohistochemistry on transverse sections at E11.5, using antibodies to TAG-1 and NFM (Figure 5). Retrograde DiI tracing of motor neuron projections was performed on E12.5 embryos by injection of DiI in forelimb muscles, but no obvious abnormality was detected in the placement of motoneuron cell bodies within the ventral horns of the mutants (data not shown). Even though we did not see major defects in peripheral sensory and motor projections, we cannot exclude that there may be more subtle defects that are not evident from this initial characterization.

In contrast to peripheral projections, when examining the central projections of sensory neurons, we observed a dramatic and fully penetrant defect at the level of the dorsal root entry zone (DREZ), the site at which the central projections of sensory neurons contact the spinal cord. Sensory afferents project to the DREZ and send axons longitudinally in the dorsal funiculus, only later, after a delay, sprouting secondary collaterals to invade the gray matter of the spinal cord (Figure 5A). The dorsal funiculus in wild-type and heterozygotes had a characteristic oval shape (Figures 5D, 5E, 5G, and 5H),

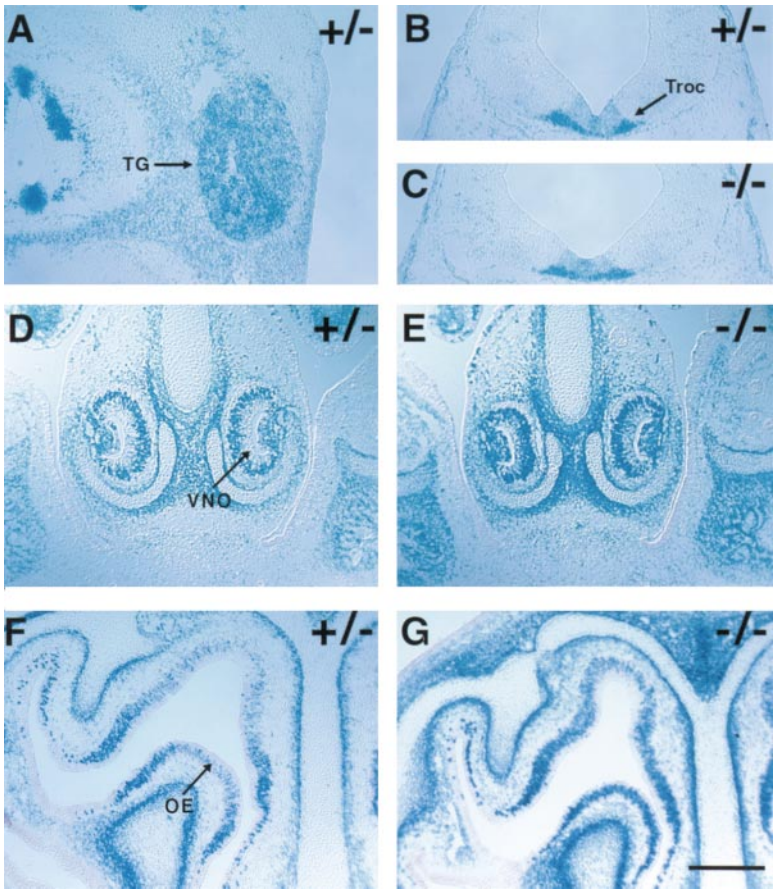

Figure 3. Expression Patterns of *neuropilin-2* Assessed by β-Galactosidase Staining

β-galactosidase staining was performed on 10 μm cryostat sections of heterozygous (+/−) and homozygous (−/−) embryos at different developmental stages to assess neuropilin-2 expression patterns and to examine morphological differences between +/− and −/− animals. All the panels are oriented with dorsal up. Scale bar, 225 μm.

(A) Horizontal section of an E11.5 +/− embryo. TG, trigeminal ganglion neurons.

(B and C) Neuropilin-2 expression in E11.5 trochlear neurons (Troc) of heterozygous (+/−) and homozygous (−/−) embryos.

(D and E) Coronal sections of +/− and −/− E19.5 embryos. VNO, vomeronasal organ.

(F and G) Coronal sections of +/− and −/− E19.5 embryos. OE, olfactory epithelium.

but in the mutants it was significantly reduced in size, and much narrower, as visualized both with NF-M staining (Figure 5F) and TAG-1 staining (Figure 5I) (in the latter case, however, the reduction was a bit obscured by the TAG-1 staining of commissural axons in the adjacent region in the dorsal spinal cord). Since *neuropilin-2* is expressed by sensory neurons at early stages, when they are beginning to project into the spinal cord (Chen et al., 1997; Figures 5B and 5C), this reduction in the size of the dorsal funiculus may reflect a cell autonomous defect in the growth or guidance of the sensory axons. Despite this decrease at E11.5, we did not observe dramatic differences in the projections of sensory axon collaterals into the spinal cord gray matter at E13.5, as visualized by injecting DiI into the DRG and allowing it to diffuse and to label the collaterals (data not shown).

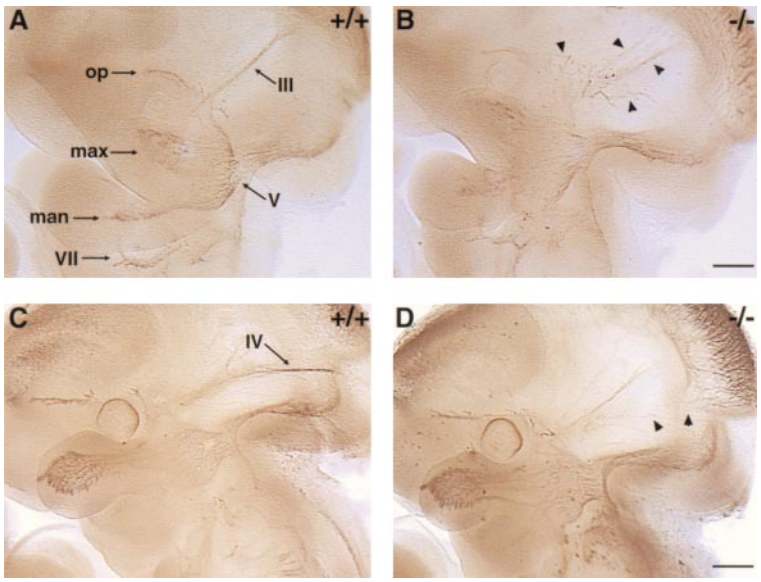

Figure 4. Peripheral Projections of Cranial Nerves in *neuropilin-2* Knockout Mice

(A and B) Whole-mount antineurofilament (NFM) staining of E10.5 embryos, showing defects in the pattern of fasciculation (arrowheads) of nerve III and the ophthalmic branch of nerve V in the mutant (−/−) (B) compared to wild-type (+/+) (A). Arrows indicate the normal pathways of cranial nerves.

(C and D) Whole-mount anti-NFM staining of E11 embryos. The trochlear nerve is missing in the mutant embryo (−/−) (D) compared to wild-type (+/+) (C). Arrowheads show the region normally traversed by the trochlear nerve.

III, oculomotor nerve; op, max, and man, ophthalmic, maxillary, and mandibular branches of the trigeminal nerve (V), respectively; IV, trochlear nerve; V, trigeminal nerve; VII, facial nerve.

Scale bar, 650 μm.

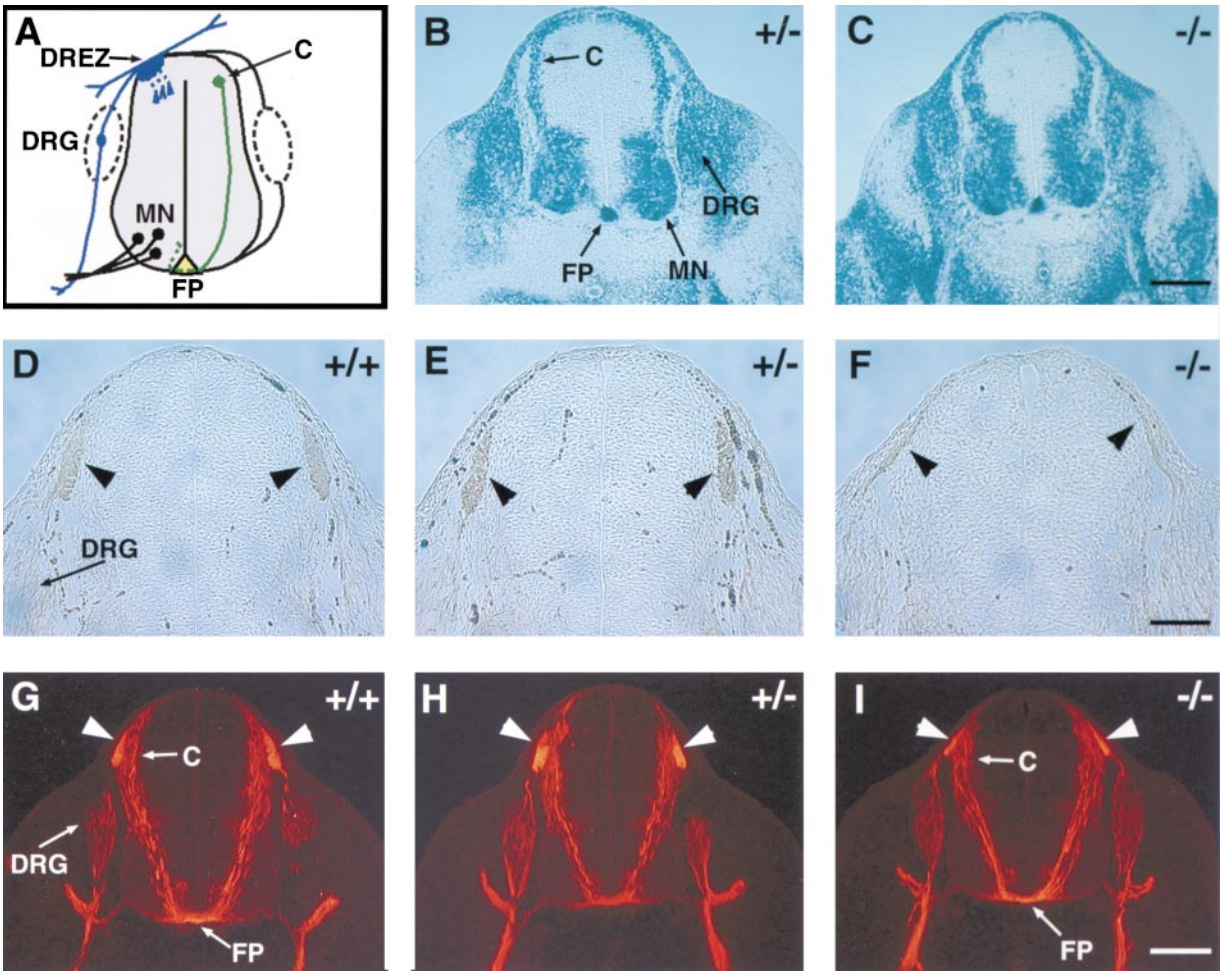

Figure 5. Defective Development of the Dorsal Funiculus in *neuropilin-2* Knockout Mice at E11.5

(A) Diagram illustrating the early projections of spinal commissural axons (C) to the floor plate (FP), of the axons of motoneurons (MN) into the periphery, and the peripheral and central projections of spinal sensory axons from cell bodies in the dorsal root ganglia (DRG). Note that the central projections develop in two stages, with axons projecting to the region of the dorsal root entry zone (DREZ) and extending in the dorsal funiculus alongside the spinal cord and then only later sprouting collaterals (dashed lines) to invade the spinal cord gray matter.

(B and C) Expression of β-galactosidase in a neuropilin-2 heterozygote (+/−) (B) and homozygote (−/−), showing that the placement of the cell bodies of *neuropilin-2*-expressing cells is apparently normal in the mutant at E11.5.

(D) through (F) The dorsal funiculus (arrowheads) is dramatically reduced in *neuropilin-2* homozygotes (−/−) (F) compared to heterozygotes (+/−) (E) or wild-type embryos (D), as visualized using an antibody to NF-M at E11.5.

(G) through (I) The defect in the dorsal funiculus at E11.5 is also evident in sections stained with an anti-TAG-1 antibody, which also illustrates that the projections of commissural axons (C) to the floor plate are largely or completely normal.

Scale bar, 220 μm for (B), (C), and (G) through (I); 110 μm for (D) through (F).

Defects in the Anterior Commissure and Habenular Tract

Neuropilin-2 mRNA is very highly expressed in all components of the olfactory and limbic systems, including the olfactory bulb, anterior olfactory nucleus, septum, piriform, and entorhinal cortices, as well as in the hippocampus (Chen et al., 1997; see below). Consistent with this, we found that β-galactosidase was very highly expressed in all these regions in both heterozygous and homozygous mice, and, further, we found that the expression patterns were identical in homozygotes and heterozygotes (data not shown; see below), indicating that the absence of the receptor does not cause marked misplacement or death of *neuropilin-2*-expressing cells. Within the olfactory system, the anterior olfactory nucleus (AON) is a major relay station, receiving collaterals from neurons in the olfactory bulb, piriform cortex, entorhinal cortex, amygdala, and AON. In turn, the AON neurons project to both the ipsilateral and controlateral main olfactory bulb and both the ipsilateral and controlateral AON. The controlateral projection of the AON forms the rostral "horseshoe-shaped" portion of the anterior commissure. As *neuropilin-2* expression is particularly strong in the AON (Figures 6A and 6B; see Chen et al., 1997), we examined whether the anterior commissure was affected in *neuropilin-2* mutant mice.

In adult mice, the anterior commissure is myelinated and can therefore be visualized by immunostaining using an antibody to myelin basic protein (MBP) (Figures 6C–6F) or by Luxol staining (data not shown). We found that in almost all cases the anterior commissure was abnormal in adult *neuropilin-2*$^{-/-}$ mice. The tract was

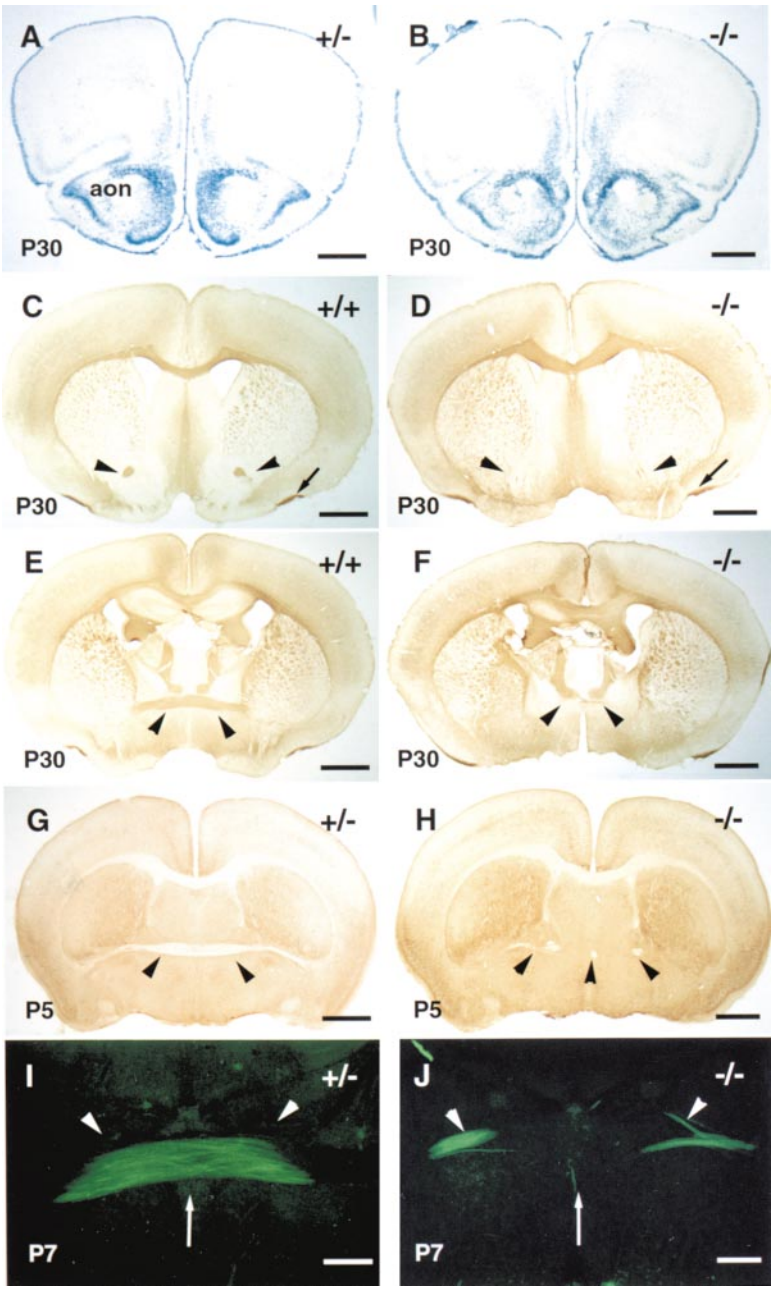

Figure 6. Defects in the Anterior Commissure in *neuropilin-2* Knockout Mice

(A and B) Coronal sections of adult mouse brain at the level of the frontal cortex and anterior olfactory nucleus processed for β-galactosidase staining. The staining pattern is identical in the +/− (A) and −/− (B) mice; in particular, β-galactosidase was very highly expressed in the anterior olfactory nucleus (AON).

(C) through (F) Immunostaining of coronal sections of adult mouse brain using an antibody to MBP reveals the presence of the anterior commissure in wild-type animals (C and E) and its absence in mutant animals (D and F). Arrowheads indicate the normal position of the anterior commissure in each section.

(G and H) Immunostaining of coronal sections of P5 animals using an antibody to CaBP reveals that the commissure is already much reduced in the mutant (H) compared to the heterozygote (G).

(I and J) High-power view of coronal sections of P7 brain labeled with anti-axonin-1 (TAG-1), showing reduction of the anterior commissure in a −/− mouse (J) compared to a +/− mouse (I). Arrow indicates the midline. Some axons still cross the midline in the mutant, but they are highly defasiculated.

Scale bar, (A) and (B), 900 μm; (C) through (F), 1 mm; (G) and (H), 800 μm; and (I) and (J), 360 μm.

either completely missing (Figures 6C–6J) or was reduced in size, with its component axon bundles defasciculated (Figure 6). Moreover, the posterior arm of the commissure, which comes from neocortical neurons, was also affected (Figure 6). This phenotype was already apparent at developmental (E19.5), neonatal (P0) (data not shown), and early postnatal stages (P5, Figures 6G and 6H; and P7, Figures 6I and 6J), as visualized by anti-TAG-1 staining, anti-calbindin staining, and hematoxilin staining (data not shown). Since, as mentioned, the size and morphology of the AON were not affected in mutant mice (Figures 6A and 6B), it seems likely that the absence of the commissure is caused by axon pathfinding errors rather than death of neurons projecting in the commissure. We were, however, unable to locate the misprojecting AON axons.

The medial habenula in the thalamus also shows extremely intense *neuropilin-2* expression (Figures 7A and 7B). Its neurons are still detected in *neuropilin-2*$^{-/-}$ mice, using β-galactosidase staining and calretinin immunostaining (Figures 7C and 7D). Habenular axons form the habenulo-interpeduncular tract, also known as the fasciculus retroflexus. By anti-MBP and Luxol staining, we found that this tract is very reduced or absent in adult *neuropilin-2* knockout mice (Figures 7E and 7F). In a few cases, the fasciculus retroflexus was still present, but its axons were highly defasiculated (data not shown).

Hippocampal Defects

Neuropilin-2 is highly expressed in the developing and adult hippocampal formation (Figures 7A and 7B; Figures 8I and 8J) and also in neurons projecting to the

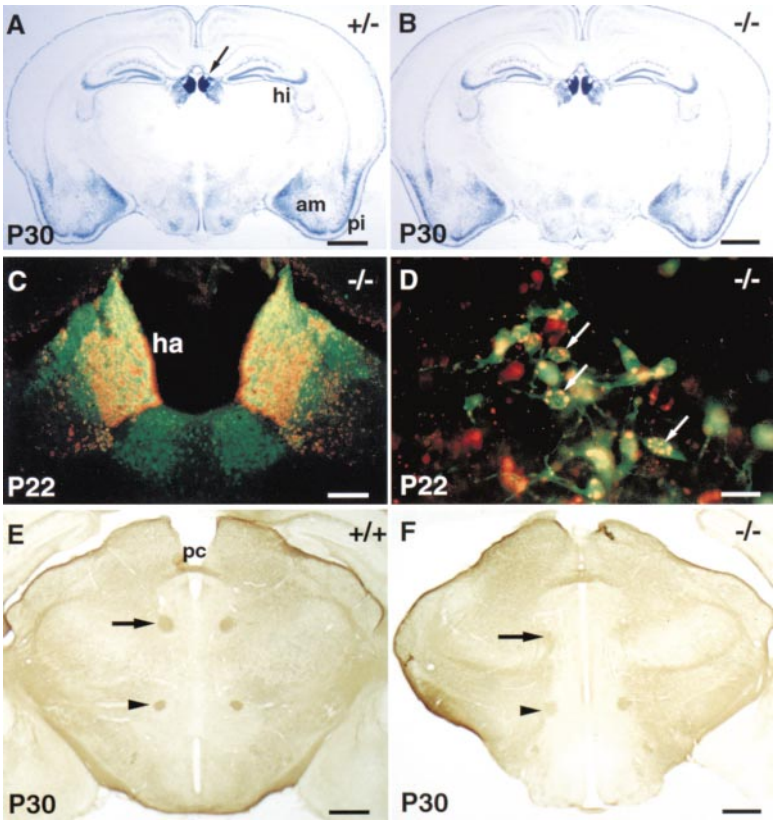

Figure 7. Defects in the Fasciculus Retroflexus in *neuropilin-2* Knockout Mice

(A and B) Coronal sections of adult mice brain processed for β-galactosidase staining, showing high expression in the medial habenula (arrow in [A]), the hippocampus (hi), the amygdala (am), and the piriform cortex (pi). The staining is identical in heterozygous (A) and homozygous (B) mice. Strong staining is also found in the meninges surrounding the brain.

(C) Coronal section at the level of the habenula of a P22 homozygote stained with anti-calretinin antibodies (FITC [green]), and anti-β-galactosidase antibodies (Texas red [red]). Neurons in the medial habenula (ha) but not in the lateral habenula strongly express *neuropilin-2*. They are covered with calretinin-positive axons of the stria medullaris (visualized with FITC).

(D) Section of the medial septum of a P22 knockout at high magnification, double-labeled for calretinin and β-galactosidase, showing that calretinin-positive septal neurons coexpress β-galactosidase. β-galactosidase staining can be seen in the cell body (arrow).

(E and F) The fasciculus retroflexus, visualized by MBP immunostaining in coronal sections of adult brain, is clearly apparent in wild-type mice (arrow in [E]) but almost completely missing in −/− mice (arrow in [F]). In contrast, the mammilothalamic tract (arrowheads in [E] and [F]) and posterior commissure (pc) are normal in the mutant.

Scale bar, (A) and (B), 1 mm; (C), 250 μm; (D), 50 μm; and (E) and (F), 580 μm.

hippocampus, such as those from the septum (Chen et al., 1997; Chédotal et al., 1998). Using β-galactosidase staining, we confirmed and extended the previous analysis of *neuropilin-2* expression in the hippocampus at embryonic and adult stages (Figures 7A and 7B; Figures 8I and 8J). During the late embryonic and early postnatal period, *neuropilin-2* is strongly expressed in the *stratum oriens* and *stratum radiatum* of the CA3, CA2, and CA1 fields, as well as in the forming pyramidal cell layer. Within the dentate gyrus, *neuropilin-2* is expressed in the dentate granule cell layer and a subpopulation of the cells in the hilus, including mossy cells. In the adult mouse, *neuropilin-2* is expressed in a portion of the pyramidal cells of CA3 and appears to be concentrated in the superficial layers of the pyramidal cell layer. *Neuropilin-2* is also expressed in occasional cells in the *stratum radiatum*. In the adult dentate gyrus, *neuropilin-2* is highly expressed in the dentate granule cell layer. There appears to be a gradient of expression that is lowest near the hilar border and highest in cells adjacent to the molecular layer (Figure 9C; data not shown), suggesting that *neuropilin-2* may be more abundant in mature than immature dentate granule cells.

The axons of embryonic neurons in the dentate gyrus, and the CA1 and CA3 regions, which all express *neuropilin-2*, have previously been shown to be repelled by both Sema3A and Sema3F (Chédotal et al., 1998; Steup et al., 1999). Using blocking antibodies, it was shown that the repulsive action of Sema3A on embryonic hippocampal axons requires neuropilin-1 function, but repulsion by Sema3F does not, and it was therefore proposed that the effect of Sema3F is mediated through a neuropilin-2-dependent mechanism (Chédotal et al., 1998). To directly investigate the requirement for neuropilin-2 in mediating the action of Sema3F on hippocampal axons, explants of dentate gyrus (DG) and CA3 neurons were microdissected from E15 and E17 embryos and were examined in vitro for their responsiveness to Sema3F in collagen gel coculture experiments. Axons emanating from explants taken from homozygous mutant embryos were not repelled by Sema3F (as observed using multiple explants from each of eight homozygotes from four litters), whereas responses to Sema3A were unaffected (Figure 8). These results establish that Sema3F-mediated repulsion of hippocampal axons requires neuropilin-2 function.

We next examined whether neuropilin-2 function is required for normal development of the hippocampus and hippocampal projections. The gross morphology of the embryonic and adult hippocampus of *neuropilin-2* mutants was indistinguishable from that of heterozygous mice (as revealed by β-galactosidase staining: Figures 7A and 7B; Figures 8J and 8I) or of wild-type mice (Figure 9; data not shown). However, a defect was detected in the projections of dentate granule cells, which normally extend axons (the mossy fibers) to the basal dendrites of the CA3 pyramidal cells in a tight bundle that travels adjacent to and above the pyramidal layer (the suprapyramidal, or main, bundle). In addition, a small fraction of the mossy fibers travel below the pyramidal layer (to form the so-called infrapyramidal bundle) but cross the pyramidal cell layer and join the main

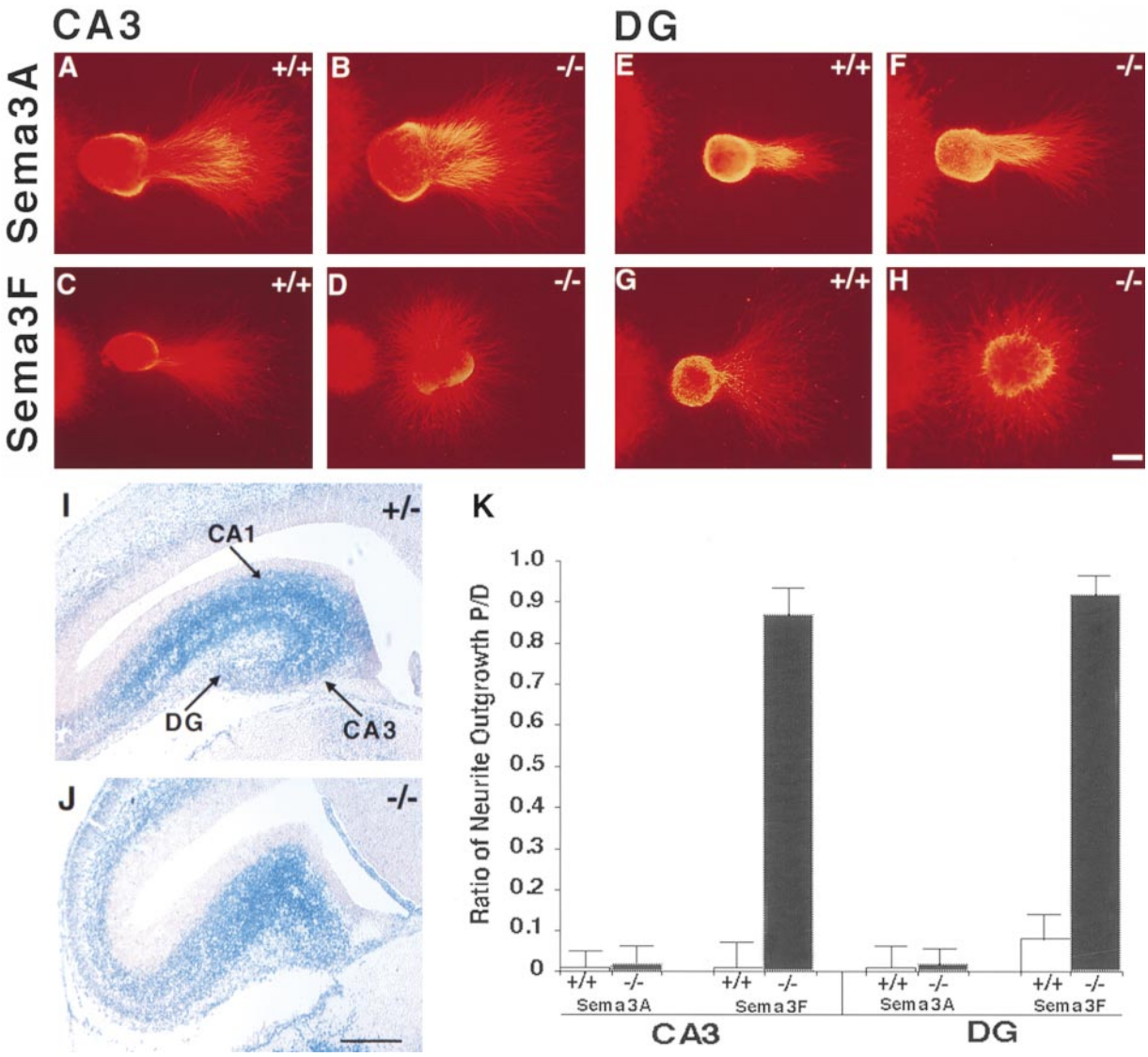

Figure 8. The Repulsive Action of Sema3F on Hippocampal Axons Requires Neuropilin-2 Function

Explants of CA3 and dentate gyrus (DG) were microdissected from E17 wild-type and mutant embryos as described by Chédotal et al. (1998) and cocultured with COS7 cells expressing Sema3A or Sema3F in collagen matrices.

(A) through (D) Responses of CA3 axons to Sema3A (A and B) and to Sema 3F (C and D). The wild-type explants (+/+) are repelled by both semaphorins (A and C), while the mutant axon (−/−) is not repelled by Sema3F (D) but is repelled by Sema3A (B).

(E) through (H) Responses of DG axons to Sema3A (E and F) and to Sema3F (G and H). DG axons from mutant embryos are repelled by Sema3A (F) but not Sema3F (H), whereas axons from wild-type embryos are repelled by both (E and G).

(I and J) β-galactosidase staining of the E17.5 hippocampus from a heterozygote (I) or a homozygote (J).

(K) Quantification of P/D ratio of neurite outgrowth as described in Figure 2. For each set of repulsion experiments, n = 16 explants were tested with Sema3A, and n = 24 explants were tested with Sema3F. Explants were obtained from 8 +/+ and −/− embryos in four separated litters. Both CA3 and DG explants from mutant embryos lose their responsiveness to Sema 3F ($p < 0.0001$ Student's test).

Scale bar, (A) through (H), 150 μm; and (I) and (J), 200 μm.

mossy fiber bundle soon after leaving the hilus. Both projections can be visualized with an antibody to calbindin or by Timm staining (which detects zinc that accumulates in mossy fiber boutons) (Figures 9A, 9B, and 9D) or with an antibody to the zinc transporter-3 (ZnT-3) (data not shown). In *neuropilin-2* homozygous mutant mice, the main mossy fiber bundle appears normal (Figures 9B and 9D). However, the fibers from the infrapyramidal bundle do not join the main bundle after leaving the hilus and instead extend underneath the pyramidal layer to the apex of the curvature of the pyramidal cell layer (Figures 9B and 9D). The presence of Timm staining in these abnormal mossy fibers suggests that they have developed mossy fiber boutons and therefore may make synaptic contact with nearby dendrites.

Another *neuropilin-2*-expressing population in the dentate gyrus is the mossy cells, located in the hilar portion of that region, which can be visualized by double staining with antibodies to calretinin and β-galactosidase (Figure 9C). In contrast to the projection of dentate granule cells, however, the projection of the mossy cells to granule cell dendrites in the controlateral dentate

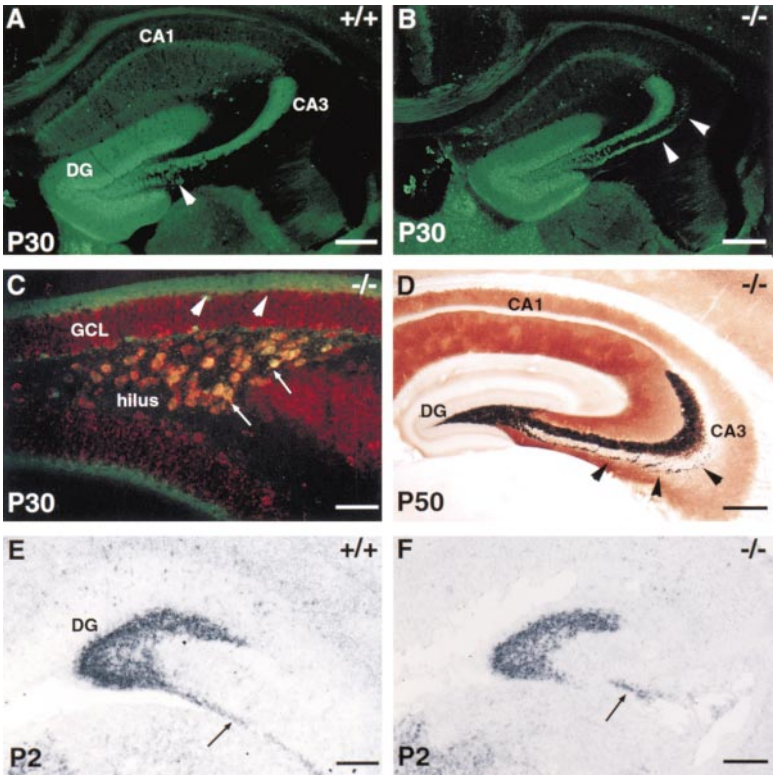

Figure 9. Altered Projection of Mossy Fibers in *neuropilin-2* Mutants

Immunostaining and histochemical staining of coronal sections of adult brains at the level of hippocampus.

(A, B, and D) Coronal sections of wild type (+/+) (A) and mutant (−/−) (B) P30 brains were labeled with anti-calbindin (FITC); coronal sections of a P50 mutant (−/−) brain was Timm stained. In the homozygote (B and D), many infrapyramidal mossy fibers abnormally extend underneath the pyramidal cell layer to the apex of the curvature of the CA3 pyramidal cell layer (arrowheads).

(C) Anti-calretinin (FITC) and anti-β-galactosidase (Texas red) double staining of a P30 mutant (−/−) brain section at high magnification. Mossy cells, in the hilar portion (hilus) of the dentate gyrus, express high level of β-galactosidase (arrows). Their calretinin positive axons (arrowheads) project onto granule cell dendrites (GCL) in the controlateral dentate gyrus. The projection appears normal in the neuropilin-2 mutant.

(E and F) Coronal sections of P2 brain showing similar expression of *Prox-1* in a wild-type (+/+) (E) and a mutant animal (−/−) (F). *Prox-1* is expressed in granule cells and cells migrating to the dentate gyrus (arrows).

DG, dentate gyrus; GCL, granule cell layer. Scale bar: (A) and (B), 600 μm; (C), 150 μm; (D), 500 μm; and (E) and (F), 250 μm.

gyrus appeared normal in the mutants (Figure 9). Since there are no convenient markers for the other afferent, efferent, and intrahippocampal pathways that may be affected following loss of *neuropilin-2* function, a more detailed characterization of these pathways in the mutant will require additional studies.

Since *neuropilin-2* is expressed in the hippocampus from the earliest stages of hippocampal development, we also examined in more detail whether there were defects in cell differentiation or migration, using a variety of histochemical and molecular markers. No marked differences in cell number, density, or position were observed between wild-type and mutant embryos by simple visual inspection of Nissl-stained sections (data not shown), although we cannot exclude the presence of more subtle defects that could be detected with more quantitative analysis. Similarly, no differences were observed between mutant and wild-type animals at late embryonic (E19) and early postnatal (P2) stages in the expression patterns of *Prox-1* (a specific marker for dentate granule cells), *Lef-1* (a specific marker for migrating immature granule cells), and *Math-2* (a specific marker for pyramidal cells), visualized by in situ hybridization on tissue sections (Figures 9E and 9F; data not shown), indicating that differentiation and migration of dentate granule cells and pyramidal cells are apparently normal in the mutant.

Several Axonal Projections of *neuropilin-2*-Expressing Cells Appear Largely Normal

As mentioned, β-galactosidase staining confirmed that *neuropilin-2* is expressed in many other neuronal populations throughout the CNS, including those in the vomeronasal organ and olfactory epithelium (Figures 3F–3I), the olfactory bulb (Figures 6A and 6B), the neocortex, the cerebellum, the motor nuclei in the hindbrain, the colliculi, and the cerebellum (Chen et al., 1997; data not shown). However, the analysis of projections to and from several of these neuronal populations did not show any noticeable defects in the absence of *neuropilin-2*. For example, axons of the lateral olfactory tracts (LOT), which are known to respond to Sema3B and Sema3F (De Castro et al., 1999), still projected normally in the knockout, as assessed by anterograde DiI tracing experiments from the olfactory bulb of E13.5–E17.5 embryos (data not shown). It is possible that redundant cues contribute to guiding these axons. For example, recent studies have shown that *Slit-2* is highly expressed in the septum and repels olfactory bulb axons in vitro (Ba-Charvet et al., 1999; Li et al., 1999); Slit-2, alone or together with other cues, may thus be sufficient to steer the axons away from the septum, even in the absence of neuropilin-2 signaling.

Discussion

Neuropilin-2 has been proposed to function as a ligand-binding moiety in receptor complexes for class 3 semaphorins, and, based on binding relations, is thought to be a necessary high-affinity receptor for the class 3 semaphorin Sema3F. Our analysis of a *neuropilin-2* knockout mouse supports this hypothesis by showing loss of Sema3F responsiveness in sympathetic and hippocampal neurons isolated from the knockout animal. Defects in several axonal projections in both the peripheral and central nervous systems in these animals also identify key roles for neuropilin-2 in axon guidance in vivo.

Isolation of a Mutant *neuropilin-2* Allele

We describe the isolation of a mutant allele of *neuropilin-2* by gene trapping, using the so-called secretory trap

vector (Skarnes et al., 1995). As in the case of a mutant *netrin-1* allele generated by the same method (Serafini et al., 1996), this allele appears to be severely hypomorphic, or near null (see the Results). Consistent with the allele being a severe loss-of-function allele, we found that sympathetic and hippocampal neurons isolated from homozygous mutant animals apparently lost entirely their responsiveness to Sema3F. Further, we did not observe any dominant effects in heterozygotes: the anatomical phenotypes we observed were fully recessive; in fact, the only phenotype we observed in the heterozygotes was a very slight decrease in responsiveness of sympathetic axons to Sema3F, again consistent with the allele being a loss-of-function allele. Finally, the phenotypes we have observed are consistent with those observed by Giger et al. (2000 [this issue of *Neuron*]), who generated a mutant allele by gene targeting, further supporting the hypothesis that this allele is a severe loss-of-function allele.

Neuropilin-2 as a Necessary Component of the Sema3F Receptor

Previous studies have led to the hypothesis that the responsiveness of different neuronal populations to different class 3 semaphorins is dictated by the complement of neuropilins expressed by responsive cells, with neuropilin-2 being required for Sema3F, Sema3B, and Sema3C responses, and neuropilin-1 for Sema3A responses. This hypothesis is supported by experiments using function-blocking antibodies to neuropilin-1 or neurons derived from neuropilin-1 knockout mice, which have shown that neuropilin-1 is required for Sema3A responses (He and Tessier-Lavigne, 1997; Kitsukawa et al., 1997; Kolodkin et al., 1997), by experiments in which neuropilin-1 or neuropilin-2 were ectopically expressed and shown to confer responsiveness to Sema3A or to Sema3B and 3C, respectively (Takahashi et al., 1998), and by experiments showing that antibodies to neuropilin-2 block sympathetic axon responses to Sema3F (Giger et al., 1998). Our results confirm and extend those studies by showing that both sympathetic and hippocampal axon responses to Sema3F are lost in neurons from *neuropilin-2* knockout mice, whereas Sema3A responses are unaffected. The Sema3F receptor is expected to require a plexin coreceptor, with plexin-A3 being a strong candidate based on its widespread expression in a variety of neuronal populations in the CNS and PNS (Takahashi et al., 1999; Tamagnone et al., 1999; data not shown).

Neuropilin-2 Is Required for Proper Projections of Oculomotor and Trochlear Axons and for Normal Development of the Dorsal Funiculus

Previous studies showed that both netrin-1 and Sema3A repel trochlear motor axons in vitro, whereas oculomotor axons are insensitive to both netrin-1 and Sema3A (Colamarino and Tessier-Lavigne, 1995; Shirasaki et al., 1996; Varela-Echavaria et al., 1997). However, the trajectories of both sets of axons are largely normal in both netrin-1 and Sema3A knockout mice (Serafini et al., 1996; Taniguchi et al., 1997) and, as expected from the Sema3A knockout phenotype, in neuropilin-1 knockout mice as well (Kitsukawa et al., 1997). *Neuropilin-2* is expressed by both trochlear and oculomotor neurons (Chen et al., 1997; this study), and we find that the axons of both neuronal populations are defective in the *neuropilin-2* knockout animals. The peripheral projections of trochlear axons are missing in E11 *neuropilin-2* mutant embryos. The trochlear motor nucleus in the ventral midhindbrain region appears normal, suggesting that the defect is in the projections of trochlear axons, although we have not yet been able to locate the misrouted axons. Consistent with the defect being one of guidance in trochlear axons, it has been shown that these axons are repelled by Sema3F (A. Kolodkin, D. Ginty, and colleagues, personal communication), and the pattern of expression of Sema3F mRNA, flanking the dorsally directed trajectory of these axons both more rostrally and more caudally (A. Kolodkin, D. Ginty, and colleagues, personal communication), is consistent with a role for Sema3F in channeling these axons along the mid-hindbrain junction. It must be assumed that there are additional cues that help set the trochlear axons off on their dorsal trajectory, and one good candidate for this is provided by members of the Slit family, which are expressed by floor plate cells and can repel at least spinal motor axons in vitro (Brose et al., 1999). In the case of oculomotor axons, the defect is apparently one of defasciculation, which is reminiscent of the defasciculation of various cranial nerve axons in the neuropilin-1 knockout mouse (Kitsukawa et al., 1997), a finding that has been interpreted as reflecting a role for Sema3A, functioning via neuropilin-1, in directing fasciculation of these axons through surround repulsion (Keynes et al., 1997; Kitsukawa et al., 1997; Taniguchi et al., 1997). Similarly, it seems likely that neuropilin-2 directs fasciculation of the oculomotor axons by interpreting a surround repulsive signal provided by Sema3F and/or other neuropilin-2 ligands. Interestingly, the cranial nerves that had severe defasiculation phenotypes in neuropilin-1 knockout mice (the ophthalmic branch and distal portions of the maxillary and mandibular portions of the trigeminal nerve [cranial nerve V], and the facial nerve [VII], glossopharyngeal nerve [IX], and vagus nerve [X]: Kitsukawa et al., 1997) were largely unaffected in the *neuropilin-2* mutant embryos, while those exhibiting no significant defects in *neuropilin-1* mutants (for instance, nerves III and IV) had severe defects in mice carrying the *neuropilin-2* mutant allele. This observation may be explained by complementary expression patterns of the two neuropilins and/or of the major ligands Sema3A and 3F in different target fields.

Another highly penetrant defect in the mutant mice was visible at E11.5 at the level of the spinal cord and involves a dramatic decrease in the size of the dorsal funiculus, where the central projections of sensory axons extend before branching into the spinal cord. The cause of this defect is unclear at present. Since sensory neurons express *neuropilin-2* at this stage, the defect may be cell autonomous and reflect a decreased growth of the central projections to or within the dorsal funiculus, although it is unclear why growth would be reduced. Whatever the cause, by E13.5 an apparently normal pattern of projection of sensory collaterals into the spinal cord is seen by DiI tracing, suggesting that there is some compensation for this early defect. Further studies will be required to determine the basis of this defect.

Major Telencephalic and Diencephalic Axonal Tracts Are Missing in *neuropilin-2* Knockout Mice

One of the most striking abnormalities detected in the CNS of the *neuropilin-2* knockout was the disorganization of the anterior commissure in the telencephalon. As mentioned, this tract has three major branches, a stria medullaris component, an anterior (or olfactory component), and a posterior (or interhemispheric) component. All these branches are affected to varying degrees in *neuropilin-2* knockout mice, and in the most extreme cases the anterior commissure was completely absent. This phenotype is reminiscent of the absence of anterior commissure in netrin-1 knockout mice (Serafini et al., 1996) and appears different from what has been observed in mice lacking the EphB2 receptor (alone or together with the EphB3 receptor), where only axons forming the posterior limb of the commissure were severely affected (Orioli et al., 1996). The mechanism by which neuropilin-2 guides anterior commissure axons during development is not clear. None of the known murine secreted semaphorins is expressed at the telencephalic midline at embryonic stages (De Castro et al., 1999), and none of the neurons contributing to the anterior commissure have yet been shown to respond to these molecules. One perhaps surprising result of our study is the apparently normal development of the lateral olfactory tract (LOT), which projects massively to neurons that contribute to the anterior commissure and whose axons are already known to respond to at least two secreted semaphorins, including Sema3F. This tract was also normal in neuropilin-1-deficient mice (Kitsukawa et al., 1997). However, LOT axons are known to be responsive to other guidance cues, such as Slit proteins (Li et al., 1999; Ba-Charvet et al., 1999), which may be sufficient to guide these axons, so that double or triple knockouts might be necessary before defects in their guidance are observed.

Another major tract affected in the *neuropilin-2* knockout mice is the fasciculus retroflexus, which is composed of habenular axons. Axons from the medial habenula project to the the interpeduncular nucleus, which is an important relay and modulatory center in the limbic and related systems. The lateral habenula component of the fasciculus retroflexus bypasses the IP and projects to the raphe nucleus. *Neuropilin-2* is very highly expressed in the medial habenula and almost absent from the lateral habenula. We found that the fasciculus retroflexus is very reduced or absent in neuropilin-2 knockouts, although in some cases a remnant of the fasciculus can still be found that might correspond to the lateral habenula component of the tract. Here again it remains to be determined how neuropilin-2 functions in guiding habenular axons, in particular which secreted semaphorins contribute to their guidance.

Tracing studies have shown that developing hippocampal axons invade their appropriate target domain and layers in a highly specific fashion (Supèr and Soriano, 1994). Such stereotyped growth suggests the involvement of both long-range cues influencing early axonal trajectories and membrane- or substrate-anchored cues, providing layer-specific positional information. It has been suggested that Sema3F may play an important role in the lamina-specific projections of hippocampal afferents (Chédotal et al., 1998). We showed here that in *neuropilin-2*$^{-/-}$ mice, hippocampal axons lose their responses to Sema3F in vitro. We also demonstrated directly a role for neuropilin-2 in hippocampal axon pathfinding in vivo. *Neuropilin-2* is normally expressed at high level in the dentate gyrus. The mossy fiber pathway, deriving from dentate granule cells, normally has two components, a main suprapyramidal bundle that travels adjacent to and above the pyramidal cell layer and a smaller infrapyramidal bundle that travels below the pyramidal layer and crosses the pyramidal cell layer to join the main mossy fiber bundle soon after leaving the hilus. The exaggerated extension of the infrapyramidal bundle in *neuropilin-2* mutant mice suggests that neuropilin-2 is necessary for the proper targeting of these fibers. A portion of these axons still cross over to join the main mossy fiber pathway but do so at greater distances than in the wild-type animal. Expression patterns for cell-type specific markers showed that cell differentiation and position are apparently normal in the mutant animals. This suggests that neuropilin-2 is largely or entirely dispensable for granule and pyramidal cell differentiation and migration and indicates that the mossy fiber defect is likely to be a primary rather than a secondary effect of the loss of *neuropilin-2*. This is consistent with neuropilin-2 playing a role in the early termination and/or crossing of axons due to neuropilin-2-mediated axon guidance by repulsion. The presence of mossy fiber boutons, as demonstrated by the presence of ZnT-3 and Timm staining in the ectopic mossy fibers, suggests that these axons make connections with other cells, which may result in the development of abnormal circuitry in these animals. It is noteworthy that several of the *neuropilin-2* phenotypes in other regions may represent partly or entirely a defasciculation, but in the mossy fiber pathway of these animals the general state of fasciculation appears to be normal. This is in contrast to previous manipulations that have been shown to disrupt mossy fiber development, the perturbation of the function of the transmembrane proteins LAMP (Pimenta et al., 1995) or NCAM (Cremer et al., 1997), which both caused dramatic defasciculation of the mossy fiber pathway. The basis of the mossy fiber phenotype of the NP-2 mutant mice is currently unclear, although there are at least three possible explanations. First, it is possible that the protein distribution of Sema3F (or that of another ligand for neuropilin-2) is more limited than the distribution of Sema3F mRNA. If this is true, then it is possible that, in the wild-type, there may be localized expression and release of a secreted short-range chemorepellant that reroutes the infrapyramidal bundle across the pyramidal layer. Second, the loss of neuropilin-2-dependent repulsive effects may uncover a permissive secreted or cell contact–dependent influence, and the unchecked positive influence from this factor may allow overgrowth of the infrapyramidal bundle. Third, neuropilin-2 may be involved in homophilic or heterophilic cell–cell interactions required for rerouting axons across the pyramidal layer in an efficient manner. Whatever the mechanism of this defect, its specificity implies that the regulation of mossy fiber axon initiation toward the CA3 region, and the decision to terminate at the CA3-CA2 border, are regulated by distinct mechanisms. Interestingly, the extent of the infrapyramidal mossy fiber projection appears to influence performance in spatial

learning and memory tasks (e.g., Schopke et al., 1991; Schwegler and Crusio, 1995). Thus, *neuropilin-2* knockout mice might provide a useful tool for the analysis of the influence of the infrapyramidal bundle on spatial learning and memory.

Neuropilin-2, as well as various semaphorin genes, continues to be expressed in the hippocampus of adult mice. The hippocampus of rodents, particularly the mossy fiber pathway, is known to be a region of high plasticity even in adulthood. In the dentate gyrus, *neuropilin-2* is highly expressed in the dentate granule cell layer, and there appears to be a gradient of expression that is lowest near the hilar border and highest in cells adjacent to the molecular layer. This corresponds to highest expression in the oldest granule cells and raises the possibility that neuropilin-2 may play a role in the ongoing plasticity associated with the mossy fiber pathway.

Conclusion

Our results provide a definitive demonstration that neuropilin-2 is a necessary receptor for mediating repulsive responses of a variety of axons to Sema3F. The defects in axonal projection patterns described here are consistent with a role for neuropilin-2 in guiding axons through repulsion, either by preventing ingrowth into inappropriate regions and/or by driving fasciculation through surround repulsion, and they provide useful tools to help dissect the mechanisms that control pathfinding of cranial nerves and major axonal tracts in the developing mammalian brain.

Experimental Procedures

Generation and Genotyping of *neuropilin-2* Mutant Mice

An E14 embryonic stem cell line containing an insertion of the secretory gene trap vector pGT1.8TM within an intron of the *neuropilin-2* gene (as assessed by 5′RACE on ES cell RNA) was generated as described (Skarnes et al., 1995). Founder chimeric males were generated and bred to CD-1, C57Bl6/J, and Sv129 females to generate heterozygous progeny. Reverse transcription (RT)-PCR was used to genotype embryos and adults. In brief, the PCR reaction used total RNA and a triple-primer set (F, 5′-AGACTACCACCCCATATCC CATGG-3′, which anneals to the cDNA; RV, 5′-CTTGAGCCTCTG GAGCTGCTCAGC-3′, which anneals to the gene trap vector; and RC, 5′-CTGCCCTGGTCCTCACGGATG-3′, which also anneals to the cDNA). PCR reactions were carried out for 35 cycles at 94°C for 1 min, 55°C for 1 min, and 72°C for 1.5 min, to yield a 432 bp wild-type band and 305 bp mutant band.

For RNase protection analysis, ^{32}P-labeled antisense riboprobes (probe A, a 250 nt fragment covered the insertion junction; probe B, a 280 nt fragment covering the 3′-end coding region of the neuropilin-2 cDNA) were transcribed using T7 RNA polymerase. RNase protection experiments were performed with 20 μg RNA and 3.2×10^5 cpm of probe using a commercially available kit (Ambion).

Explant Culture and Whole-Mount Staining

Superior cervical ganglia and hippocampal neuron explants were dissected from E13.5 embryos or E15.5-E17.5 embryos, respectively, and cocultured with COS7 cell aggregates expressing Sema3A or Sema3F in three-dimension collagen matrices for 48 hr, and then fixed and immunostained with an anti-NFM antibody or anti-β-tubulin antibody as described (Chédotal et al., 1998; Chen et al., 1998). Whole-mount immunostaining using an anti-NFM antibody on E10.5 and E11 embryos was performed as described (Kitsukawa et al., 1997).

Immunocytochemistry

Brains were processed for immunohistochemistry as described (Chédotal et al., 1998) and stained with one or more of the following antibodies: mouse monoclonal against neurofilament (NFM) (1:300); mouse monoclonal against myelin basic protein ([MBP] 1:1000, Euromedex); mouse monoclonal against calbindin-D_{28K} (1:10000, kindly provided by Dr. W. Hunziker) (Celio, 1990); rabbit polyclonal against β-galactosidase (1:1500, Cappel, Cooper Biomedical); rabbit polyclonal against calbindin-D_{28K} (1:8000, Swant, Bellinzona, Switzerland); goat polyclonal against calretinin (1:1500, Swant); goat polyclonal against chick axonin-1/TAG-1 (1:1000); or antibody against the Zinc-Transporter-3 (ZnT-3) (1:100; generously provided by Dr. R. Palmter). Sections were rinsed and then incubated for 1 hr with one or more of the following secondary antibodies: a biotinylated horse anti-mouse antibody (1:200, Vector) or a biotinylated goat anti-rabbit antibody (1:200, Vector), followed by streptavidine-HRP (1:400, Amersham); or with FITC conjugated-donkey anti-goat antibody (1:100, Nordic) and a Texas Red-conjugated donkey anti-rabbit antibody (1:100, Amersham); or a FITC-conjugated sheep anti-mouse antibody (1:50. Amersham) and a Cy3-conjugated goat anti-rabbit antibody (1:200; Jackson Immunoresearch); or a FITC-conjugated sheep anti-rabbit (1:100, Silenus, Melbourne, Australia) and a Cy3-conjugated goat anti-mouse antibody (1:200; Jackson Immunoresearch).

In Situ Hybridization

In situ hybridization probes for Prox-1 and Math-2 were generated by RT-PCR using the following primers: for Prox-1, TCTTAAGCCGG-CAAACCAAGAGGA and TTGCTCCTGGAAAAGGCATCATGG; and for Math-2, TGTTAACACTACCGTTTGACG and AGCATCATTGAGG-CCGTGCAT. The Lef-1 probe was a gift of Dr. R. Grosschedl.

Timm Staining

Tissue preparation and processing was performed according to the modified Timm's procedure described by Sloviter (1982). Nissl staining was performed on 5 μm thick paraffin embedded tissue as described by Parent et al. (1999).

Acknowledgments

We thank F. Roger and J. Mak for technical assistance. H. C. is supported by a National Institutes of Health fellowship. S. J. P. is supported by a Howard Hughes Medical Institute postdoctoral fellowship for physicians. Supported by a National Institutes of Health grant (to W. C. S.), by the INSERM APEX and ARC (to A. C.), and by the International Spinal Research Trust (to M. T. L.). W. C. S. is a Searle Scholar, and M. T. L. is an Investigator of the Howard Hughes Medical Institute.

Received November 4, 1999; revised November 23, 1999.

References

Brose, K., Bland, K.S., Wang, K.H., Arnott, D., Henzel, W., Goodman, C.S., Tessier-Lavigne, M., and Kidd, T. (1999). Slit proteins bind Robo receptors and have an evolutionarily conserved role in repulsive axon guidance. Cell *96*, 795–806.

Celio, M.R. (1990). Calbindin D-28k and parvalbumin in the rat nervous system. Neuroscience *35*, 375–475.

Chédotal, A., Del Rio, J.A., Ruiz, M., He, Z., Borrell, V., de Castro, F., Ezan, F., Goodman, C.S., Tessier-Lavigne, M., Sotelo, C., and Soriano, E. (1998). Semaphorins III and IV repel hippocampal axons via two distinct receptors. Development *125*, 4313–4323.

Chen, H., Chédotal, A., He, Z.-G., Goodman, C.S., and Tessier-Lavigne, M. (1997). Neuropilin-2, a novel member of the neuropilin family, is a high affinity receptor for the semaphorins Sema E and Sema IV but not Sema III. Neuron *19*, 547–559.

Chen, H., He, Z.-G., Bagri, A., and Tessier-Lavigne, M. (1998). Semaphorin-neuropilin interactions underlying sympathetic axon responses to class III semaphorins. Neuron *21*, 1283–1290.

Chisholm, A., and Tessier-Lavigne, M. (1999). Conservation and divergence of axon guidance mechanisms. Curr. Opin. Neurobiol. *9*, 603–615.

Colamarino, S.A., and Tessier-Lavigne, M. (1995). The axonal chemoattractant netrin-1 is also a chemorepellent for trochlear motor axons. Cell *81*, 621–629.

Comeau, M.R., Johnson, R., DuBose, R.F., Petersen, M., Patrick, G., VandenBos, T., Park, L., Farrah, T., Mark Bullar, R., Cohen, J.I., et al. (1998). A poxvirus-encoded semaphorin induces cytokine production from monocytes and binds to a novel cellular semaphorin receptor, VESPR. Immunity *8*, 473–482.

Cremer, H., Chazal, G., Goridis, C., and Represa, A. (1997). NCAM is essential for axonal growth and fasciculation in the hippocampus. Mol. Cell Neurosci. *8*, 323–335.

De Castro, F., Hu, L., Drabkin, H., Sotelo, C., and Chedotal, A. (1999). Chemoattraction and chemorepulsion of olfactory bulb axons by different secreted semaphorins. J. Neurosci. *19*, 4428–4436.

Giger, R.J., Urquhart, E.R., Gillespie, S.K., Levengood, D.V., Ginty, D.D., and Kolodkin, A.L. (1998). Neuropilin-2 is a receptor for semaphorin IV: insight into the structural basis of receptor function and specificity. Neuron *21*, 1079–1092.

Giger, R.J., Cloutier, J.-F., Sahay, A., Prinjha, R.K., Levengood, D.V., Moore, S.E., Picering, S., Simmons, D., Rastan, S., Walsh, F.S., et al. (2000). Neuropilin-2 is required in vivo for selective axon guidance responses to secreted semaphorins. Neuron *25*, this issue, 29–41.

Goodman, C.S., Kolodkin, A.L., Luo, Y., Püschel, A.W., and Raper, J.A. (1999). Unified nomenclature for the semaphorins/collapsins. Cell *97*, 551–552.

He, Z.-H., and Tessier-Lavigne, M. (1997). Neuropilin is a receptor for the axonal chemorepellent semaphorin III. Cell *90*, 739–751.

Kawakami, A., Kitsukawa, T., Takagi, S., and Fujisawa, H. (1996). Developmentally regulated expression of a cell surface protein, neuropilin, in the mouse nervous system. Neurobiology *29*, 1–17.

Kawasaki, T., Kitsukawa, T., Bekku, Y., Matsuda, Y., Sanbo, M., Yagi, T., and Fujisawa, H. (1999). A requirement for neuropilin-1 in embryonic vessel formation. Development *126*, 4895–4902.

Keynes, R., Tannahill, D., Morgenstern, D.A., Johnson, A.R., Cook, G.M., and Pini, A. (1997). Surround repulsion of spinal sensory axons in higher vertebrate embryos. Neuron *18*, 889–897.

Kitsukawa, T., Shimizu, M., Sanbo, M., Hirata, T., Taniguchi, M., Bekku, Y., Yagi, and Fujisawa, H. (1997). Neuropilin-semaphorin III/D-mediated chemorepulsive signals play a crucial role in peripheral nerve projection in mice. Neuron *19*, 995–1005.

Kolodkin, A.L. (1998). Semaphorin-mediated neuronal growth cone guidance. Prog. Brain Res. *117*, 115–132.

Kolodkin, A.L., Levengood, D.V., Rowe, E.G., Tai, Y.-T., Giger, R.J., and Ginty, D.D. (1997). Neuropilin is a semaphorin receptor. Cell *90*, 753–762.

Li, H.-S., Chen, J.-H., Wu, W., Fagaly, T., Zhou, L., Yuan, W., Dupuis, S., Jiang, Z.-H., Nash, W., Gick, C., et al. (1999). Vertebrate slit, a secreted ligand for the transmembrane protein roundabout, is a repellent for olfactory bulb axons. Cell *96*, 807–818.

Makinen, T., Olofsson, B., Karpanen, T., Hellman, U., Soker, S., Klagsbrun, M., Eriksson, U., and Alitalo, K. (1999). Differential binding of vascular endothelial growth factor B splice and proteolytic isoforms to neuropilin-1. J. Biol. Chem. *274*, 21217–21222.

Migdal, M., Huppertz, B., Tessler, S., Comforti, A., Shibuya, M., Reich, R., Baumann, H., and Neufeld, G. (1998). Neuropilin-1 is a placenta growth factor-2 receptor. J. Biol. Chem. *273*, 22272–22278.

Nakamura, F., Tanaka, M., Takahashi, T., Kalb, R.G., and Strittmatter, S.M. (1998). Neuropilin-1 extracellular domains mediate semaphorin D/III-induced growth cone collapse. Neuron *2*, 1093–1100.

Nguyen Ba-Charvet, K., Brose, K., Marillat, V., Kidd, T., Goodman, C.S., Tessier-Lavigne, M., Sotelo, C., and Chédotal. A. (1999). Slit-2-mediated chemorepulsion and collapse of developing forebrain axons. Neuron *22*, 463–473.

Orioli, D., Henkemeyer, M., Lemke, G., Klein, R., and Pawson, T. (1996). Sek4 and Nuk receptors cooperate in guidance of commissural axons and in palate formation. EMBO J. *15*, 6035–6049.

Parent, M., Levesque, M., and Parent, A. (1999). The pallidofugal projection system in primates: evidence for neurons branching ipsilaterally and contralaterally to the thalamus and brainstem. Chem. Neuroanat. *16*, 153–165.

Pimenta, A.F., Zhukareva, V., Barbe, M.F., Reinoso, B.S., Grimley, C., Henzel, W., Fischer, I., and Levitt, P. (1995). The limbic system-associated membrane protein is an Ig superfamily member that mediates selective neuronal growth and axon targeting. Neuron *15*, 287–297.

Schopke, R., Wolfer, D.P., Lipp, H.P., and Leisinger-Trigona, M.C. (1991). Swimming navigation and structural variations of the infrapyramidal mossy fibers in the hippocampus of the mouse. Hippocampus *1*, 315–328.

Schwegler, H., and Crusio, W.E. (1995). Correlations between radial-maze learning and structural variations of septum and hippocampus in rodents. Behav. Brain Res. *67*, 29–41.

Serafini, T., Colamarino, S.A., Leonardo, E.D., Wang, H., Beddington, R., Skarnes, W.C., and Tessier-Lavigne, M. (1996). Netrin-1 is required for commissural axon guidance in the developing vertebrate nervous system. Cell *87*, 1001–1014.

Shirasaki, R., Mirzayen, C., Tessier-Lavigne, M., and Murakami, F. (1996). Guidance of circumferentially growing axons by netrin-dependent and -independent floorplate chemotropism in the vertebrate brain. Neuron *17*, 1079–1088.

Skarnes, W.C., Moss, J.E., Hurtley, S.M., and Beddington, R.S. (1995). Capturing genes encoding membrane and secreted proteins important for mouse development. Proc. Natl. Acad. Sci. USA *92*, 6592–6596.

Soker, S., Takashima, S., Miao, H.Q., Neufeld, G., and Klagsbrun, M. (1998). Neuropilin-1 is expressed by endothelial and tumor cells as an isoform-specific receptor for vascular endothelial growth factor. Cell *92*, 735–745.

Steup, A., Ninnemann, O., Savaskan, N.E., Nitsch, R., Puschel, A.W., and Skutella, T. (1999). Semaphorin D acts as a repulsive factor for entorhinal and hippocampal neurons. Eur. J. Neurosci. *11*, 729–734.

Supèr, H., and Soriano, E. (1994). The organization of the embryonic and early postnatal murine hippocampus. II. Development of entorhinal, commissural, and septal connections studied with the lipophilic tracer DiI. Comp. Neurol. *344*, 101–120.

Takagi, S., Hirata, T., Agata, K., Mochii, M., Eguchi, G., and Fujisawa, H. (1991). The A5 antigen, a candidate for the neuronal recognition molecule, has homologous to complement component and coagulation factors. Neuron *7*, 295–307.

Takagi, S., Kasuya, Y., Shimizu, M., Matsuura, T., Tsuboi, M., Kawakami, A., and Fujisawa, H. (1995). Expression of a cell adhesion molecule, neuropilin, in the developing chick nervous system. Dev. Biol. *170*, 207–222.

Takahashi, T., Nakamura, F., Jin, Z., Kalb, R.G., and Strittmatter, S.M. (1998). Semaphorins A and E act as antagonists of neuropilin-1 and agonists of neuropilin-2 receptors. Nat. Neurosci. *1*, 487–493.

Takahashi, T., Fournier, A., Nakamura, F., Wang, L.-H., Murakami, Y., Kalb, R.G., Fujisawa, H., and Strittmatter, S.M. (1999). Plexin-neuropilin-1 complexes form functional semaphorin-3A receptors. Cell *99*, 59–69.

Tamagnone, L., Artigiani, S., Chen, H., He, Z., Ming, G.-L., Song, H.-J., Chedotal, A., Winberg, M.L., Goodman, C.S., Poo, M.-M., et al. (1999). Plexins are a large family of receptors for transmembrane, secreted, and GPI-anchored semaphorins in vertebrates. Cell *99*, 71–80.

Taniguchi, M., Yuasa, S., Fujisawa, H., Naruse, I., Saga, S., Mishina, M., and Yagi, T. (1997). Disruption of semaphorin III/D gene causes severe abnormality in peripheral nerve projection. Neuron *19*, 519–530.

Tessier-Lavigne, M., and Goodman, C.S. (1996). The molecular biology of axon guidance. Science *247*, 1123–1133.

Varela-Echavaria, A., Tucker, A., Puschel, A.W., and Guthrie, S. (1997). Neuron *18*, 193–207.

Winberg, M.L., Noordermeer, J.N., Tamagnone, L., Comoglio, P.M., Spriggs, M.K., Tessier-Lavigne, M., and Goodman, C.S. (1998). Plexin A is a neuronal semaphorin receptor that controls axon guidance. Cell *95*, 903–916.